J Mol Model (2011) 17:1091–1108
DOI 10.1007/s00894-010-0812-7

ORIGINAL PAPER

DFT modeling on the suitable crown ether architecture for complexation with Cs^+ and Sr^{2+} metal ions

Anil Boda · Sk. Musharaf Ali · Madhav R. K. Shenoi · Hanmanth Rao · Sandip K. Ghosh

Received: 28 January 2010 / Accepted: 14 July 2010 / Published online: 30 July 2010

Abstract Crown ether architectures were explored for the inclusion of Cs^+ and Sr^{2+} ions within nano-cavity of macrocyclic crown ethers using density functional theory (DFT) modeling. The modeling was undertaken to gain insight into the mechanism of the complexation of Cs^+ and Sr^{2+} ion with this ligand experimentally. The selectivity of Cs^+ and Sr^{2+} ions for a particular size of crown ether has been explained based on the fitting and binding interaction of the guest ions in the narrow cavity of crown ethers. Although, Di-Benzo-18-Crown-6 (DB18C6) and Di-Benzo-21-Crown-7 (DB21C7) provide suitable host architecture for Sr^{2+} and Cs^+ ions respectively as the ion size match with the cavity of the host, but consideration of binding interaction along with the cavity matching both DB18C6 and DB21C7 prefers Sr^{2+} ion. The calculated values of binding enthalpy of Cs metal ion with the crown ethers were found to be in good agreement with the experimental results. The gas phase binding enthalpy for Sr^{2+} ion with crown ether was higher than Cs metal ion. The ion exchange reaction between Sr and Cs always favors the selection of Sr metal ion both in the gas and in micro-solvated systems. The gas phase selectivity remains unchanged in micro-solvated phase. We have demonstrated the effect of micro-solvation on the binding interaction between the metal ions (Cs^+ and Sr^{2+}) and the macrocyclic crown ethers by considering micro-solvated metal ions up to eight water molecules directly attached to the metal ion and also by considering two water molecules attached to metal-ion-crown ether complexes. A metal ion exchange reaction involving the replacement of strontium ion in metal ion-crown ether complexes with cesium ion contained within a metal ion-water cluster serves as the basis for modeling binding preferences in solution. The calculated O-H stretching frequency of H_2O molecule in micro-solvated metal ion-crown complexes is more red-shifted in comparison to hydrated metal ions. The calculated IR spectra can be compared with an experimental spectrum to determine the presence of micro-solvated metal ion–crown ether complexes in extractant phase.

Keywords DFT · IR spectra · Macrocyclic crown ethers · Micro-solvation

A. Boda · S. M. Ali (✉) · M. R. K. Shenoi · H. Rao · S. K. Ghosh
Chemical Engineering Group, Bhabha Atomic Research center, Mumbai 400085, India
e-mail: musharaf@barc.gov.in

Introduction

Macrocyclic crown ethers have drawn much experimental and theoretical interest since they were first described by Pederson in 1967 [1] and still a lot of work is being pursued. These cyclic polyethers can form remarkably stable complexes with different metal cations. Furthermore, the selectivity of this binding is sensitive to macrocyclic ring size, ether-heteroatom, and substituent. By changing the size of the ring; the donor atoms such as O, N, S, or P; and the substituent; the properties of the ligand can easily be tuned. Introduction of additional methylene to rigid crown ether to change the molecular symmetry is a new way to design and synthesize highly selective host ligands. The chiral recognition property of crown ethers upon complexation [2] can be used to develop simple enzyme-like catalysis. Fixing long hydrophobic chains onto crown ether can be used for self-organization of the macrocycles [3]. The relative ease of preparation of a broad range of derivatives makes crown ethers attractive targets for both

theoretical and applied studies [4–6]. Because of their host-guest complexation and molecular recognition properties, crown ethers have proved to be useful in sensing [7], switching [8], phase transfer catalysis [9], extraction [10], and chromatography [11, 12]. Crown ethers have also been used as membrane-forming amphiphiles [13], as biometric receptors [14], and because of their ionophoretic properties, as model ion channels [15]. The selectivity of complexation of metal ions in crown ether is poorly understood [16, 17]. It has usually been interpreted in terms of the size of the crown ether's cavity and the size of the guest ion [18]. This suggests that the most stable complexes would be formed by crown ethers and ions that match in size. On the other hand, it should be kept in mind that the stability of the complexes formed depends to a great extent on the nature of the electron donor atoms present in the ligand and micro-solvation of metal ions in aqueous phase. The selection of the donor atoms in the crown ethers can be guided by the well-known Hard-and-soft-acids-and-bases (HSAB) principle [19, 20]. The hard and soft cations are stably complexed by hard and soft electron donors, respectively. The objective of the present effort is to study the factors that control the binding selectivity and efficiency of ligating species that are important in the pretreatment of nuclear and chemical wastes. We have studied the binding mechanism of metal ion with crown ether ligands, useful to aid cleanup of mixed wastes that contain radionuclides such as cesium (Cs^{+}) and strontium (Sr^{2+}), and other transuranic metal ions.

Research in metal ion separation chemistry concentrates on the structure, energetic and thermodynamics of ion-ligand complexes (such as crown ethers) and the dynamics of complex formation in aqueous solutions. The chemistry of the cesium ion is different from the chemistry of strontium ion in solution. The Cs^{+} ion has a low charge density due to its large ionic radius and low charge. As a result, the energy associated with bond formation between the cesium ion and the functional groups of the organic extractants is typically insufficient to completely dehydrate the cation and to strip away the water molecules associated with the anion that must accompany the cation into the organic phase to maintain electrical neutrality [21]. Several experimental [22–35] approaches have been taken in the art to enhance the liquid/liquid separation of cesium and Sr ions by crown ethers. Regarding the selection of the crown ether extractant, the following points are very important: (i) branched side chains on crown ether benzo derivatives increase the solubility of the extractant in the organic phase (ii) the strongest ion binding by a crown ether occurs when the ion fits best into the crown ether cavity (iii) 21-Crown-7 is the appropriate size for cesium ions. To the best of our knowledge, no critical and exhaustive assessment of Cs^{+} and Sr^{2+} selective ligands from a theoretical point of view has been performed.

Experimental procedures are very time consuming and laborious in general and in particular, special care should be taken for handling radioactive elements. In view of this the most suitable alternative for fast screening of solvent and extractant before carrying out the actual experiments is the molecular modeling based computational approach which has now become very supportive for prediction of structures, reaction mechanism, partitioning behavior of extractant and so on. Molecular modeling using computational chemistry is perhaps the most powerful tool for the design and study of complex molecular systems and interpretation of their stabilities and other properties. The microscopic details and physical properties of a large molecular system like cavity of the macrocyclic crown ether, its shape and dimension, sites for ion pairing and ion-dipole and dipole-dipole interaction with the guest metal ion can be confidently predicted using advanced computational [36–39] methods.

Computational and theoretical models [39] of the complex molecular processes, which occur in solution and liquid/solid interfaces require highly reliable and quantitative values for both gases as well as for liquid phases. Accurate experimental values of such fundamental quantities such as gas phase metal ion-ether bond dissociation enthalpies would provide an ideal component to theoretical predictions. Unfortunately, very few of the experimental studies conducted over past several decades have attempted to measure this quantity [40–43]. Extensive computational works [44–71] have been done on the conformational structure of the crown ether and its interaction with various metal ions either in the gas phase or in presence of the solvent. The optimized structures and binding energy for Cs complexes of 12-Crown-4, 15-Crown-5 and 18-Crown-6 have been reported using RHF/6-31 + G* and MP2/6-31 + G* levels of theory [72]. The optimized geometries and binding energies of Cs-anisole complexes have been reported at RHF/6-311G* and MP2/6-311 + G* levels of theory [73]. Recently, the structures and binding enthalpies for Cs complexes with 12-crown-4, 15-Crown-5 and 18-Crown-6 at HF/6-31 + G* and B3LYP/6-31 + G* levels of theory have been reported [74]. The suitable ligand architecture with appropriate cavity size for Cs and Sr metal ions is not well studied. Also, a simple clear concept beyond the host-guest size complementarities and structural rigidity has not been exploited significantly in designing host ligands. In the past, electrostatic interactions of cations with negatively charged atoms (O or N) in host ligands have been harnessed extensively as the main criteria for designing novel host ligands, while the energetically favored orientations of the dipoles toward the cation have not been seriously exploited. Also a correlation between the binding energy and charge obtained from Mulliken population analysis for host guest type of interaction was scarcely studied. Our endeavor

here will be to predict suitable ligand architecture for Cs and Sr metal ions based on the structure, energetic and thermodynamics of the crown ether metal ions complexes using DFT based molecular modeling approach.

Computational protocol

All calculations of metal ion-crown ether complex systems were performed with the B3LYP, which is one of the most popular and extensively used hybrid functionals implemented in the frame of DFT computational calculations. DFT is capable of providing adequately accurate structures and thermodynamical properties of different molecular systems [75]. Among various density functional modules, the Becke's three-parameter nonlocal hybrid exchange correlation functional B3LYP (Becke-Lee-Yang-Parr) density functional is quite well studied [76–80]. Geometry optimization for M^{n+}-ether complexes has been performed with the B3LYP density functional using cc-PVDZ basis function for H and O atoms; cc-PVTZ for carbon and 3-21G split valence basis set for Cs^{+} and Sr^{2+} metal ions. In order to find out the most stable equilibrium structure of M^{+}-ether complexes, the initial guessed structures obtained from PM3 semi-empirical calculation were used followed by full geometry optimization procedure without imposing any symmetry restrictions as implemented in GAMESS suite of quantum chemistry code [81]. The optimized minimum energy structure has been confirmed by the absence of any imaginary frequency in the hessian calculation. The same hessian output has been used for the thermodynamic data generation. We have used MOLDEN program for the visualization of various molecular geometries [82] and calculation of different structural parameters for free and metal ion-complexed crown ethers. BSSE correction was also performed using full counterpoise method [83].

Thermal corrections to the electronic energy (E_{el}), enthalpy (H) and free energy (G) of the optimized free crown ethers and metal ion-crown ether complexes have been performed following the earlier reported procedure [84, 85]. The total internal energy (U) of free crown ethers and metal ion-crown ether complexes is obtained after adding the correction term (CT) to the electronic energy as

$$U = E_{el} + CT, \tag{1}$$

where CT is defined as

$$CT = E_{trans} + E_{rot} + E_{vib}(T). \tag{2}$$

Here, E_{trans}, E_{rot} and E_{vib} represent the energy contribution from translational, rotational and vibrational motions [84] respectively. T is the absolute temperature. The corrected enthalpy in the ideal gas approximation using standard thermodynamic relation, $H = U + PV$ (work term) can be expressed as

$$H = U + RT, \tag{3}$$

with the corrected free energy as

$$G = H - TS. \tag{4}$$

Here, R represents the universal gas constant and S is the total entropy of the system obtained from the sum of translational, rotational and vibrational contributions.

Results and discussion

The fully equilibrated structures of crown ethers, various structural and energy parameters, molecular descriptors and thermodynamic parameters with different ring size and donor O atoms are presented here. The representative metal ions considered here are Cs^{+} and Sr^{2+} ion due to their significance in the nuclear waste management. Details on the predicted structures and calculated results are provided in the following sections. Schematic representations of crown ether ligands under study are displayed in Fig. 1.

Structural parameters

Unsubstituted crown ether

The fully relaxed minimum energy structures of the unsubstituted host (crown ether) ligands of increasing ring size due to increment of O donor atom are displayed in Fig. 2a. In 12-Crown-4 (12C4), two O atoms placed

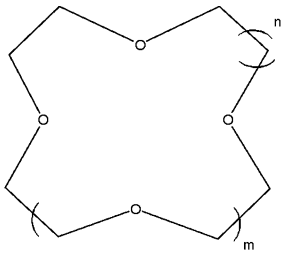

m=1, 2, 3, 4, 5 and n=1 : 12C4, 15C5, 18C6, 21C7 and 24C8

n= 2, 3, 4, 5 and m=1 : 13C4, 14C4, 15C4 and 16C4

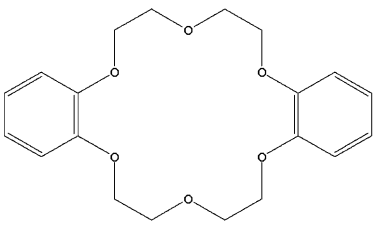

DB18C6

Fig. 1 Schematic representations of various free, extended and benzo substituted crown ether

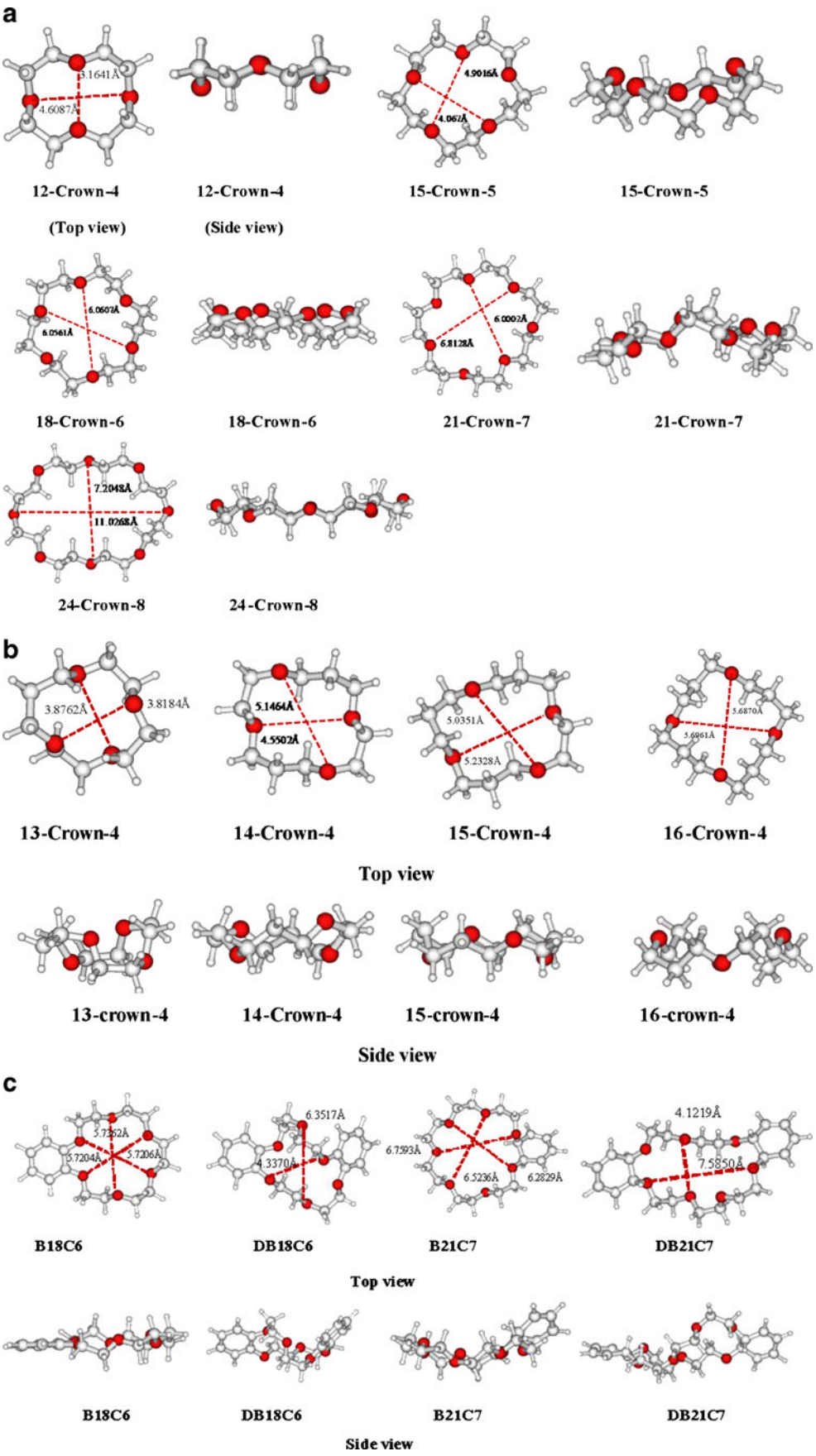

Fig. 2 **a.** Fully optimized minimum energy structure at B3LYP level of theory using cc-PVDZ basis function for H and O atom, cc-PVTZ basis function for C atom of free crown ether ligand: 12-crown-4, 15-crown-5, 18-crown-6, 21-crown-7 and 24-crown-8. The largest red spheres, medium sized grey spheres and smallest grey spheres refer to O atom, C atom and H atom respectively. **b.** Fully optimized minimum energy structure at same level of theory as in Fig. 2a of free crown ether ligand: 13-crown-4, 14-crown-4, 15-crown-4 and 16-crown-4. **c.** Fully optimized minimum energy structure at same level of theory as in Fig. 2a of free crown ether ligand: benzo-18-crown-6, di-benzo-18-crown-6, benzo-21-crown-7 and di-benzo- 21-crown-7

diagonally are at the top of the ring and two O atoms are at the bottom of the crown ring. For 15-Crown-5 (15C5), four adjacent O atoms are lying on the top and the remaining one is projected inward of the ring, whereas all six O atoms sit at the top of the crown plane in 18-Crown-6 (18C6). Five O atoms are projected at the top and two O atoms are projected at the bottom of the crown plane in 21-Crown-7 (21C7), whereas, eight O atoms in 24-Crown-8 (24C8) are placed in an alternate up and down position. Large number of conformers can be generated by tuning the dihedral angle of crown ethers. Conformation search is altogether a different and difficult study in view of the floppy nature of the crown ethers. Hence, the initial input structures for most stable conformer of 12C4, 15C5, 18C6 and 21C7 were taken from earlier reported results [86].

Tuned extended crown ether

The crown ethers mentioned above are substantially soluble in water, which is not desirable for the experimentalist in the separation experiments. The structure can be altered by adding alkyl or phenyl groups within the ring or as a substituent which in turn reduce the solubility of the crown ether in water and hence enhances the extraction capability. Our aim here is to tune the structure of the crown ether either by varying the $–CH_2$-CH_2- link with longer alkyl chains or phenyl ring within the basic crown ring. In the first case, the cavity of the crown ring can be tuned by extending the ring with the addition of methylene linkage ($–CH_2$- unit) within the crown ether ring. This effect is studied by considering the 12C4 unit as the basic unit (because it is the simplest and less floppy crown ether) and addition of each $–CH_2$- unit leads to 13C4, 14C4, 15C4 and 16C4 crowns, for which optimized structures are displayed in Fig. 2b.

Tuned benzo substituted crown ether

The structure of the host crown ether can also be altered by phenyl ring instead of $–CH_2$-CH_2- link within the crown ether moiety. This effect is studied for 18C6 and 21C7 crown ethers. Optimized structures for these substituted crown ethers are shown in Fig. 2c. In Benzo-18C6, due to the addition of one benzene ring within the crown ring the structure becomes slightly distorted but addition of one more benzene substituent causes a strong deformation on the structures of Di-Benzo-18C6. Similar effects occur in case of Benzo-21C7 and Di-Benzo-21C7 also.

Metal ion-crown ether complexes

Unsubstituted crown ether

The fully optimized minimum energy structures of unsubstituted crown ether with Cs^+ and Sr^{2+} metal ions are displayed in Fig. 3a and b respectively. After complexion with metal ion, the center to center O-O distance (between two opposite atoms) becomes smaller due to strong electrostatic interaction of the metal ion with the crown oxygen electron density in comparison to the free crown ether as shown in Table 1a. From the figure it is seen that Cs^+ metal ion sits at the top of the crown ether plane from 12C4 to 18C6 and is fully encapsulated in the cavity of 21C7. Again, it moves from the crown ether plane in case of 24C8. The diameter of Cs^+ and Sr^{2+} ion are 3.38 Å and 2.26 Å respectively. The Sr^{2+} metal ion is completely encapsulated in the cavity of 18C6 due to its appropriate size matching within the cavity than Cs which is larger in size than the crown ether cavity as clearly demonstrated in Fig. 2b (detailed analysis of crown ether cavity has been discussed in later section). However, for 21C7 and 24C8 the structure is squeezed due to strong force field of the Sr^{2+} metal ion. The Cs-O and Sr-O metal ion crown ether bond distance is increased gradually due to increased cavity size of the crown ether as seen in Table 2a.

Tuned extended crown ether

In order to search for suitable cavity architectures for Cs and Sr metal ions, the complex of these metal ions with extended crown ether has also been optimized and the resulted structures are displayed in Fig. 4a and b for Cs and Sr respectively. The cavity of the crown ethers becomes smaller due to strong electrostatic interaction of the metal ion with the crown oxygen electron density in comparison to the uncomplexed crown ether as shown in Table 1b. Due to the extended ring, the cavity size is increased and hence the Cs-O bond distance also increases but Sr-O bond distance decreases as seen in Table 2b. This is attributed to smaller size and higher charge on Sr metal ion in comparison to Cs metal ion. Note, recently, interaction of this extended crown ether with lithium and sodium metal ion has been reported [87].

Tuned benzo substituted crown ether

Next, we demonstrate the effect of benzo substitution in the crown ether ring since the cavity size can also be adjusted by the attachment of phenyl ring in the crown ether moiety. Benzo group plays an opposite effect in comparison to the effect of –CH2-O-CH2- unit or $–CH_2$-CH_2-CH_2- unit within the crown ether ring. The optimized structures for Cs and Sr metal ion complexes with the benzo substituted crown ether are displayed in Fig. 5a and b respectively. The optimized structures of Cs complexes are symmetric in nature for all the benzo substituted crown ethers B18C6, DB18C6, B21C7 and DB21C7 studied here. Among these Cs is best fitted in the cavity of DB21C7 crown moiety. The

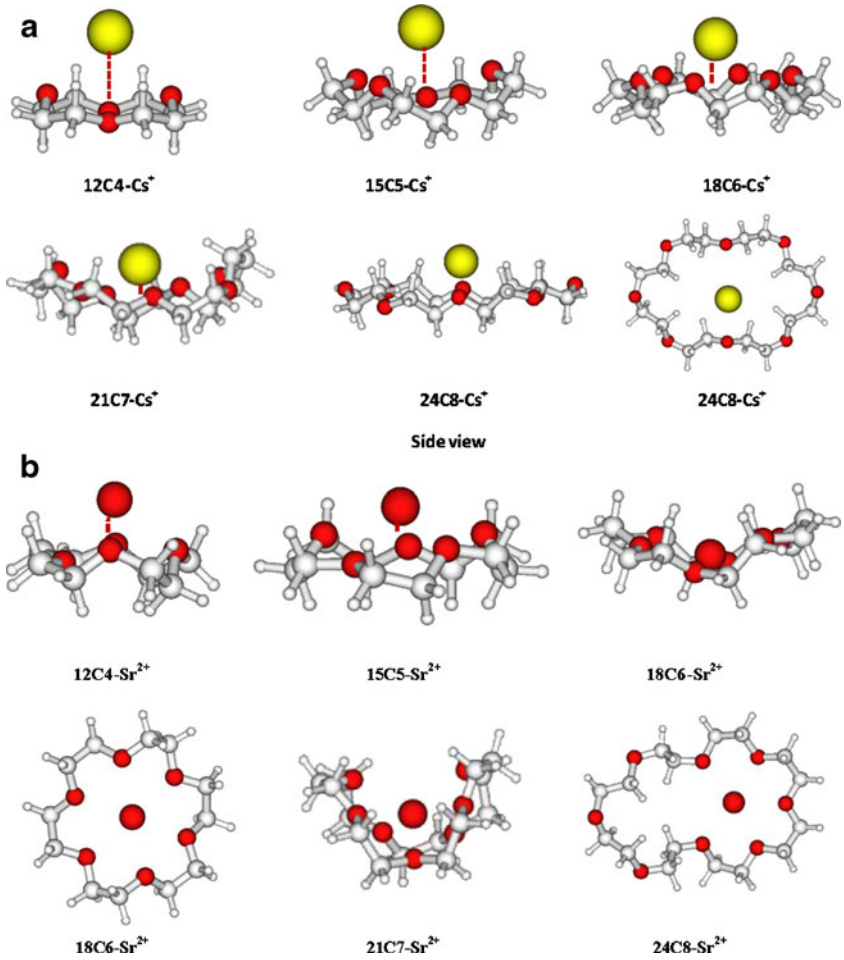

Fig. 3 **a.** Fully optimized minimum energy structures of Cs^+ ion-crown ether complexes at B3LYP level of theory using cc-PVDZ basis function for H and O atom, cc-PVTZ basis function for C atom and 3-21G basis function for Cs atom. The yellow sphere represents the Cs^+ metal ion. **b.** Fully optimized minimum energy structures of Sr^{2+} ion-crown ether complexes at B3LYP level of theory using cc-PVDZ basis function for H and O atom, cc-PVTZ basis function for C atom and 3-21G basis function for Sr atom. The red sphere represents the Sr^{2+} metal ion

optimized structures of Sr complexes are symmetric for B18C6 and DB18C6 but become distorted for B21C7 and DB21C7 due to strong electronic polarization effect of doubly charged Sr metal ion. The cavity of the crown ether, i.e., the center to center O-O distance (between two opposite O atoms) becomes smaller due to strong electrostatic interaction of the metal ion with the crown oxygen electron density in comparison to the un-complexed crown ether as shown in Table 1c. The Cs-O and Sr-O metal ion crown ether bond distance is decreased gradually with decrease in cavity size of the crown ether as seen in Table 2c.

Micro-solvated metal ion-crown ether complexes

It is commonly believed that during transfer of metal ions from an aqueous solution to the organic phase, the metal ion is not completely dehydrated, it is accompanied by one or two water molecules in the extractant phase. Hence, it is of importance to study the effect of hydrated metal ion in micro-solvated metal ion-crown ether complexes and its impact on structure and binding interaction with ligand molecules. In order to study the effect of micro-solvated metal ion on ion exchange reaction, the micro-solvated metal ion and its crown complexes have been optimized and are displayed in Fig. 5b. In the case of DB18C6-Sr^{2+}-$(H_2O)_2$ complexes, strontium ion is coordinated to all six ethereal O atoms as well as two additional O atoms from two H_2O molecules in a distorted cubic geometry. Similar structure for DCH18C6-Sr^{2+}-$(H_2O)_2$ has been reported earlier in EXAFS experiment [88]. The structural parameters are displayed in Table 3. The distance between Sr metal ion and the ethereal O atom (Sr-O (min.)= 2.5919 Å, Sr-O (max.) = 2.7041 Å) has been lengthened slightly from the unsolvated metal complex. Similarly, in DB21C7-Sr^{2+}-$(H_2O)_2$ complex, strontium ion is coordinated to all seven ethereal O atoms as well as two additional O atoms from two H_2O molecules. The distance between Sr metal ion and the ethereal O atom (Sr-O (min.)=2.6800 Å), Sr-O (max.) = 2.8935 Å) has been increased from the unsolvated metal complex. The distance between Sr metal ion and the O atom of water molecule attached to DB18C6 crown ether (Sr-O (min.) = 2.6029 Å, Sr-O (max.) = 2.6085 Å) is increased from the di-hydrated metal cluster (Sr-O=2.5470 Å). The distance between Sr metal ion and the O atom of water molecule attached to DB21C7 crown ether (Sr-O (min.)=2.6640 Å and Sr-O (mix.) =2.6975 Å) is also higher in comparison to the hydrated metal cluster.

Table 1 Calculated structural parameters of metal ion ligand ($M^{n+}L$) systems at B3LYP level of theory using cc-PVDZ basis function for H and O atom, cc-PVTZ basis function for C atom and 3-21G basis function for Cs and Sr atom

System ($M^{n+}L$) M^{n+}= Cs^+, Sr^{2+} L	Center to center O-O diagonal distance in Å free crown ether		Center to center O-O diagonal distance in Å Cs^+-L complex		Center to center O-O diagonal distance in Å Sr^{2+}-L complex		Average cavity size(Å) calculated	Average cavity size(Å) Experiment
	Minimum	Maximum	Minimum	Maximum	Minimum	Maximum		
a) Unsubstituted crown ether								
12C4	3.16	4.60	2.95	4.52	3.60	4.10	1.24	1.2-1.5
15C5	4.06	4.90	3.93	4.91	4.00	4.62	1.84	1.7-2.2
18C6	6.05	6.06	5.87	5.87	5.14	5.19	3.41	2.6-3.2
21C7	6.00	6.95	6.19	6.49	4.26	5.16	3.84	3.4-4.2
24C8	7.20	11.02	6.07	11.01	4.15	9.74		
b) Extended crown ether								
13C4	3.81	3.87	3.82	4.43	3.54	4.32	1.21	1.1-1.4*
14C4	4.55	5.14	4.35	4.48	3.93	5.14	2.20	
15C4	5.03	5.23	4.04	5.45	4.06	4.51	2.49	
16C4	5.68	5.69	4.97	5.56	4.41	4.41	3.05	
c) Benzo substituted crown ether								
B18C6	5.72	5.73	5.17	5.64	5.14	5.25	3.06	
B21C7	6.28	6.78	6.27	6.43	4.26	5.14	3.89	
DB18C6	4.33	6.35	5.50	5.61	5.08	5.21	2.70	
DB21C7	4.12	7.58	5.83	6.37	3.78	5.27	3.20	

* Reference [98]

Table 2 Calculated structural parameters of metal ion ligand ($M^{n+}L$) systems at B3LYP level of theory using cc-PVDZ basis function for H and O atom, cc-PVTZ basis function for C atom and 3-21G basis function for Cs and Sr atom

System ($M^{n+}L$) L	Bond length Cs^+-O (Å)		Bond length Sr^{2+}-O (Å)		Dipole moment free crown ether (Debye)
	Minimum	Maximum	Minimum	Maximum	
a) Unsubstituted crown ether					
12C4	3.18	3.20	2.47	2.56	0.785
15C5	3.08	3.24	2.51	2.61	3.218
18C6	3.28	3.29	2.61	2.63	5.490
21C7	3.20	3.39	2.60	2.70	2.083
24C8	3.36	3.44	2.56	2.61	0.417
b) Extended crown ether					
13C4	3.16	4.43	2.46	2.57	0.684
14C4	3.24	3.26	2.47	2.52	0.168
15C4	2.97	4.73	2.46	2.52	0.820
16C4	3.38	4.91	2.47	2.49	0.008
c) Benzo substituted crown ether					
B18C6	3.09	3.26	2.59	2.65	1.727
B21C7	3.30	3.34	2.58	2.68	2.041
DB18C6	3.12	3.28	2.56	2.67	1.472
DB21C7	3.10	3.29	2.57	2.69	3.056

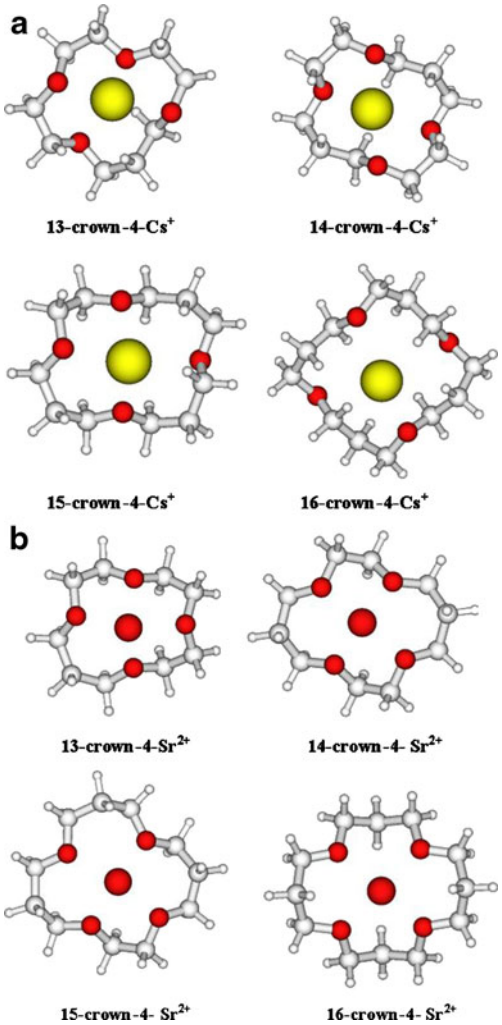

Fig. 4 **a.** Fully optimized minimum energy structures of Cs^+ ion-crown ether complexes at the same level of theory as in Fig. 3a. The yellow sphere represents the Cs^+ metal ion. **b.** Fully optimized minimum energy structures of Sr^{2+} ion-crown ether complexes at the same level of theory as in Fig. 3b. The red sphere represents the Sr^{2+} metal ion

Cavity size of free crown ethers

Unsubstituted crown ether

In order to get an idea about the inclusion of a metal cation in crown ethers cavity, the knowledge of cavity size (center to center distance between two opposite O atoms) is of great practical importance. The cavity size of the crown ether is calculated by subtracting the oxygen diameter (2.64 Å) from the center to center distance between two opposite O atoms of the crown ether [89]. The selectivity of crown ethers for various metal ions is determined by the correspondence of the metal ion size and the size of the crown ether cavity. Calculated values of cavity size for free crown ethers and metal ion crown ether complexes are listed in Table 1a. The cavity size is increased with increase in the ring size from 12C4 to 21C7. The calculated average cavity size of 12C4, 15C5, 18C6 and 21C7 is in good agreement with the reported experimental values [90]. The cavity size of free crown ethers becomes more rigid after complexation with metal ions as revealed from the center to center O-O distance (between two opposite O atoms) in metal ion –crown ether complexes. In the case of 24C8, the shape of the crown ether obtained in the present study is

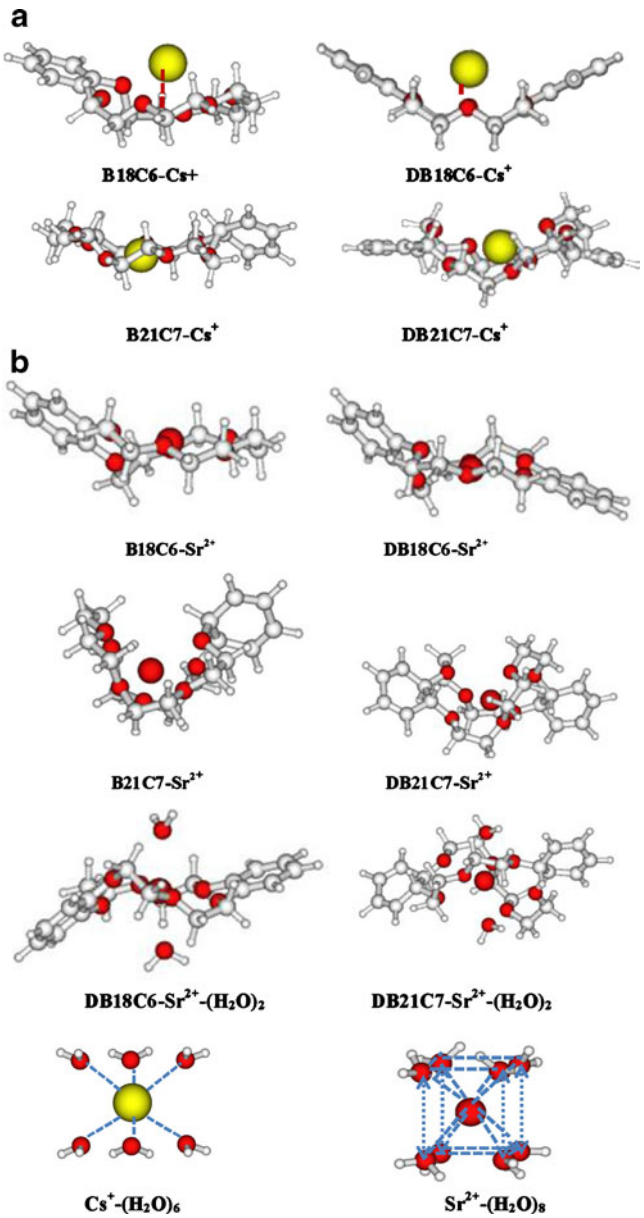

Fig. 5 **a.** Fully optimized minimum energy structures of Cs^+ ion-crown ether complexes at the same level of theory as in Fig. 3a.The yellow sphere represents the Cs^+ metal ion. **b.** Fully optimized minimum energy structures of Sr^{2+} ion-crown ether complexes at the same level of theory as in Fig. 3b. Also displayed are the optimized structures of di-benzo-18-crown-6-$2H_2O$, di-benzo-21-crown-7-$2H_2O$, Cs^+-$(H_2O)_6$ and Sr^{2+}-$(H_2O)_8$. The red sphere represents the Sr^{2+} metal ion

Table 3 Calculated values of different structural and thermodynamical parameters of hydrated metal ion ligand (M^+L-nH_2O, n=1, 2) system at B3LYP level of theory using cc-PVDZ basis function for H and O atom, cc-PVTZ basis function for C atom and 3-21G basis function for Sr atom

System	Bond length r_{M-O} (Å)				ΔU (kcal/mol)	ΔH (kcal/mol)	Charge (a.u.)
	Crown ligand		H_2O				
	Min.	Max.	Min.	Max.			
Sr^{2+}-H_2O			2.51		-44.62	-45.22	1.9193
Sr^{2+}-$2H_2O$			2.54		-86.92	-87.52	1.8356
DB18C6-Sr^{2+}-$2H_2O$	2.59	2.70	2.60	2.60	-145.66	-146.25	1.4020
DB21C7-Sr^{2+}-$2H_2O$	2.68	2.89	2.66	2.69	-157.01	-157.61	1.3400

cylindrical type and hence average cavity size cannot be predicted. The cavity diameter of 12C4, 15C5 and 18C6 is smaller than the diameter of Cs^+ ion (3.38 Å) and hence cannot accommodate Cs^+ ion in the cavity. The cavity diameter of 21C7 is 3.84 Å and can easily accommodate the Cs^+ ion. The cavity diameter of 12C4 and 15C5 is smaller than the diameter of Sr^{2+} ion (2.26 Å) and hence cannot accommodate Sr^{2+} in the cavity. The cavity diameter of 18C6 (3.41 Å) and 21C7 (3.84 Å) is sufficient to accommodate the Sr^{2+} ion.

Tuned extended crown ether

The cavity size can also be tuned with the addition of -CH_2- unit in the crown ether ring. The calculated value of cavity size is increased with increase in the ring size due to addition of –CH_2- unit in the free crown ethers from 13C4, 14C4, 15C4 and 16C4 respectively in comparison to the cavity size of 12C4 as reflected in Table 1b. The increment in the crown ether cavity due to the addition of methylene unit is small in comparison to the addition of extra ether linkage in 12C4. The cavity diameter of 13C4 and 14C4 though has increased substantially still smaller than that of Sr^{2+} ion diameter. The cavity of 15C4 and 16C4 is large enough to accommodate the Sr^{2+} ion. The cavity diameter is increased from 1.24 Å for 12C4 to 3.04 Å for 16C4 but still smaller than that of Cs^+ ion size. There is an increment of 145.16% cavity size in going from 12C4 to 16C4.

Tuned benzo substituted crown ether

The tuning of the crown ether cavity size was done by the addition of phenyl ring which imparts rigidity to the crown moiety. The calculated value of cavity size is reduced due to the replacement of –CH2-CH2- link with phenyl ring. The average cavity sizes for B18C6 and DB18C6 are less than the cavity size of 18C6 crown ether. The cavity size reduction is 10.26% in B18C6 and 20.82% in DB18C6. Though the average cavity size in B21C7 is almost unchanged in comparison to its free counterpart, 21C7, the average cavity size in DB21C7 is reduced by 16.66% in comparison to the value of cavity size in 21C7 crown ether.

Binding energy

Calculated values of internal energy (U) of metal ion-crown ether complexes are presented in Table 4a and b after thermal and zero point energy corrections. Since crown ethers with narrow cavity are excellent host in trapping charged selective metal ions from a mixture of metal ions, the most important property to be studied is the gas phase binding energy (BE), i.e., in absence of any solvent water molecules. The B.E (ΔU) of M^+-ether complex for the metal ion (M^+)-crown ether ligand (L) complexation reaction,

$$M^+ + L = M^+L, \tag{5}$$

is defined by the following general relation,

$$\Delta U = E^+_{M-ether} - \left(E^+_M + E_{ether}\right), \tag{6}$$

where, $E^+_{M\text{-}ether}$, E^+_M and E_{ether} refer to the energy of M^+-ether complex, M^+ ion and the free ether system respectively. The BSSE corrected values of binding energies are presented in Table 5. The contribution from BSSE is not significant except in the case of Cs complexes of 24C8 and DB18C6. It is expected that binding energy should be lowered after BSSE correction. In a few cases the binding energy is found to be higher after BSSE correction and was reported earlier [91].

Unsubstituted crown ether

The calculated values of binding energies for both Cs^+ and Sr^{2+} metal cations with unsubstituted crown ethers are plotted in Fig. 6a. The calculated values of binding energy for Cs metal ion are in good agreement with the experimental results. The binding energy is enhanced from 12C4 to 21C7 and then reduced in 24C8 crown for both

Table 4 Calculated thermodynamic parameters of metal ion ligand ($M^{n+}L$) systems at B3LYP level of theory using cc-PVDZ basis function for H and O atom, cc-PVTZ basis function for C atom and 3-21G basis function for Cs and Sr atom. The temperature considered here is 298.15 K

System	ΔU Kcal/mol	ΔS cal/mol	ΔH Kcal/mol	ΔG Kcal/mol
(**a**)				
Cs^+-unsubstituted crown ether				
12C4	-19.96	-30.29	-20.55	-11.52
15C5	-36.13	-24.94	-36.73	-29.29
18C6	-46.93	-28.13	-47.53	-39.14
21C7	-50.27	-26.08	-50.87	-43.09
24C8	-8.41	-38.87	-9.01	2.58
Cs^+-extended crown ether				
13C4	-19.15	-26.63	-19.75	-11.81
14C4	-18.17	-27.87	-18.77	-10.46
15C4	-22.82	-25.26	-23.42	-15.89
16C4	-12.93	-24.86	-13.53	-6.11
Cs^+-benzo substituted crown ether				
B18C6	-41.91	-31.56	-42.51	-33.10
B21C7	-50.04	-34.99	-50.63	-40.20
DB18C6	-43.32	-24.83	-43.92	-36.51
DB21C7	-40.79	-29.07	-41.38	-32.71
(**b**)				
Sr^{2+}-unsubstituted crown ether				
12C4	-122.88	-34.27	-123.48	-113.26
15C5	-155.92	-29.35	-156.52	-147.77
18C6	-183.97	-41.27	-184.56	-172.26
21C7	-200.63	-43.06	-201.23	-188.39
24C8	-164.03	-39.13	-164.62	-152.95
Sr^{2+}-extended crown ether				
13C4	-133.57	-30.28	-134.17	-125.14
14C4	-145.43	-35.47	-146.03	-135.45
15C4	-177.85	-32.64	-178.44	-168.71
16C4	-155.57	-34.57	-156.16	-145.85
Sr^{2+}-benzo substituted crown ether				
B18C6	-177.79	-39.91	-178.39	-166.49
B21C7	-206.48	-45.11	-207.08	-193.63
DB18C6	-172.95	-32.22	-173.54	-163.93
DB21C7	-198.09	-43.45	-198.69	-185.73

Cs^+ and Sr^{2+} metal cations. The increase in binding energy from 12C4 to 21C7 may be explained by the increased dipole moment of the ligand due to more O donor atom (except 21C7, where the value is smaller than 15C5 and 18C6) and increased charge transfer on the metal ion (highest in 21C7) in crown complexes. In the case of 24C8 the binding energy is lowered though one more O donor atom is added to 21C7. This may be explained as follows. First, the dipole moment of the 24C8 is quite small, 0.417. Second, in the metal ion-complex only two O donor atoms are within the interaction zone and remaining six O donor atoms are far apart from the central metal cation. Third, the charge transfer from the metal ion to the crown ring is very small. This can be understood from the Mullikan charge population analysis. The calculated values of Mullikan charge on the metal ion in crown complexes are given in Table 5a and also in Fig. 7a. The charge transfer is increased from 12C4 to 21C7 and then dropped in 24C8. The interaction energy of strontium ion with crown ethers is always higher than cesium ion due to higher charge than cesium ion. The interaction energy is increased by 144.14% for Cs^+ ion and 69.21% for Sr^{2+} in going from 12C4 to 21C7.

Tuned extended crown ether

Now, the focus is given to the effect of tuned expanded ring size on the binding energy due to the addition of methylene

Table 5 Calculated energy parameters and charge of metal ion ligand ($M^{n+}L$) systems at B3LYP level of theory using cc-PVDZ basis function for H and O atom, cc-PVTZ basis function for C atom and 3-21G basis function for Cs and Sr atom

System	Binding energy (Kcal/mol)			Charge on the metal cation (a.u)	
	Cs^+	Exp.	Sr^{+2}	Cs^+	Sr^{2+}
a) Unsubstituted crown ether					
12C4	-22.38(-23.04)	-20.57±2.15	-120.57(-125.50)	0.9265	1.7407
15C5	-40.47(-37.14)	-24.16±1.43	-161.94(-163.72)	0.9057	1.6977
18C6	-49.99(-46.76)	-40.66±2.15	-188.67(-196.48)	0.887	1.6491
21C7	-54.64(-51.48)	-	-204.02(-216.24)	0.8688	1.5583
24C8	-7.83(-10.83)	-	-167.42(-170.98)	0.9278	1.6585
b) Extended crown ether					
13C4	-19.40(-19.58)	-	-136.94(-139.96)	0.9304	1.7327
14C4	-17.36(-17.59)	-	-146.50(-148.33)	0.9335	1.7073
15C4	-23.11(-24.25)	-	-151.41(-154.20)	0.9296	1.6941
16C4	-15.02(-14.28)	-	-154.71(-157.56)	0.9483	1.6660
c) Benzo substituted crown ether					
B18C6	-45.99(-41.45)	-	-183.80(-186.38)	0.8921	1.6531
DB18C6	-45.75(-37.77)	-32.53±8.37	-179.06(-182.06)	0.9070	1.6687
B21C7	-56.13(52.69)	-	-213.42(-213.65)	0.8693	1.5141
DB21C7	-54.94(-47.31)*	-	-214.33(212.44)*	0.8689	1.4762

Values in ( ) are BSSE corrected

* Calculated using GAMESS - V. 9.0 (USA).

(-CH2-) linkage within the crown ether ring. The predicted values of binding energy are gradually decreased from 12C4 to 16C4 except 15C4 in the case of Cs^+ metal complexes as displayed in Fig. 6b. This may be due to decrease in dipole moment of the crown ether from 12C4 to 16C4 except 15C4, where it is increased. The decrease in biding energy is also reflected in the continuous increase of the metal ion-oxygen bond distance from 12C4 to 16C4 except 15C4, where it is decreased. The charge transfer from the metal ion to the crown ring becomes small in going from 12C4 to 16C4 except 15C4. This can be understood from the Mullikan charge population analysis. The calculated values of Mullikan charge on the metal ion in crown complexes are given in Table 5b. The charge transfer is decreased from 12C4 to 16C4 and then enhanced in 15C4. Though the values of binding energy are decreased in the case of Cs metal ion, the predicted values of binding energy are gradually increased from 12C4 to 16C4 in Sr metal complexes except 15C4 where it is highest. In C4 homologous series, 15C4 shows the maximum binding energy for both the Cs^+ and Sr^{2+} metal ions. This is due to the decrease in metal oxygen bond distance as one goes from 12C4 to 16C4. Also the charge transfer from metal ion to the crown moiety is increased as revealed from the Mullikan charge population analysis presented in Table 5b and Fig. 7b. The interaction energy of strontium ion with crown ethers is always higher than cesium ion due to higher charge than cesium ion. The interaction energy is decreased by 32.88% for Cs^+ ion whereas it is increased by 38.85% for Sr^{2+} in going from 12C4 to 16C4.

Tuned benzo substituted crown ether

To explore the effect of phenyl ring on the binding energy due to replacement of CH2-CH2- unit within the crown ring, the interaction of metal ions with substituted crown ethers was also studied. The calculated values of binding energy are decreased from 18C6 < B18C6 < DB18C6 and are given in Fig. 6c. The introduction of phenyl moiety decreases the stability of 18C6 and hence reduces the complexing ability as reflected in the calculated values of binding energy. The dipole moment is also decreased in the same order, 18C6 < B18C6 < DB18C6. The transfer of charge from the metal ion to the crown moiety also follows the same trend. Similar trend has also been observed for Sr metal ion complexes. In going from 21C7 to DB21C7, the binding energy is decreased due to the introduction of phenyl moiety which decreases the stability of 18C6 and hence reduces the complexing ability. Here, the dipole moment is decreased from 21C7 to B21C7 but is increased in DB21C7. The transfer of charge from the Cs metal ion to the crown moiety is decreased gradually from 21C7 to DB21C7 but is reversed for Sr metal ion. For Cs, the effect is quite substantial whereas binding energy change is very small for Sr metal complexes as shown in Table 5c. For a particular crown ether the binding energy is much higher for Sr metal ion in comparison to the singly charged large Cs metal ion. Doubly charged and small sized Sr metal ion causes a greater polarization on the crown moiety than Cs metal ion. This is reflected in the smaller Sr-O distance than Cs-O distance and also the higher charge transfer for Sr-crown complexes than Cs-crown complexes as reflected

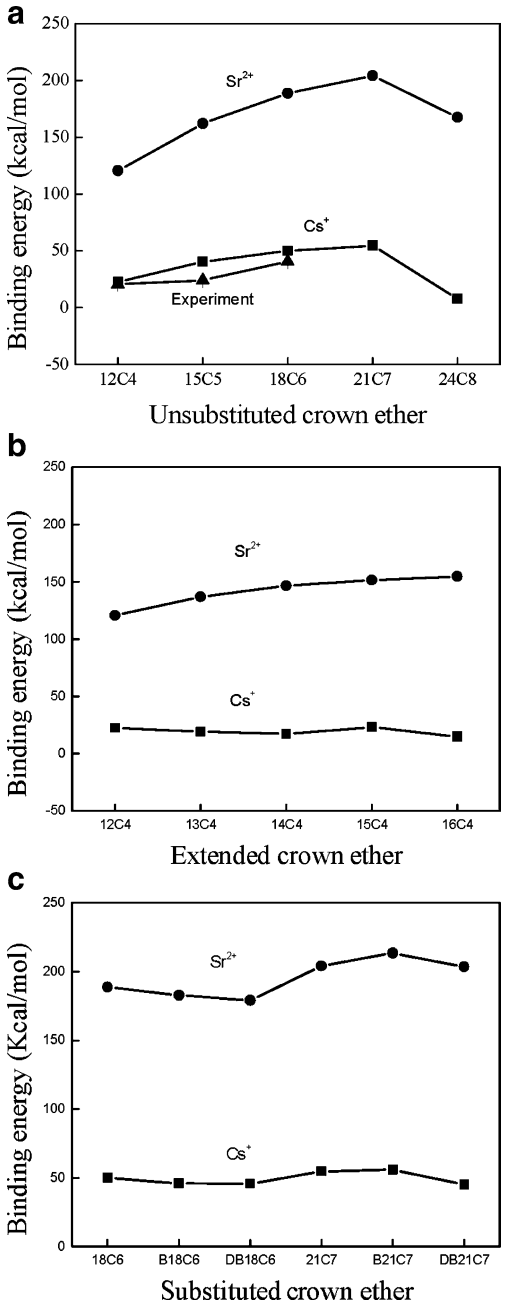

Fig. 6 **a**. Plot of calculated binding energy (BE) versus ring size of unsubstituted crown ether at B3LYP level of theory using cc-PVDZ basis function for H and O atom, cc-PVTZ basis function for C atom and 3-21G basis function for Cs and Sr atom in metal ion- crown ether complexes. Filled black square and circle represent the results obtained from the present DFT calculation for Cs and Sr ion respectively whereas filled triangle represents the experimental results for Cs. **b**. Plot of calculated binding energy (BE) versus ring size of extended crown ether at same level of theory as in Fig. 6a in metal ion- crown ether complexes. Filled black square and circle represent the results obtained from the present DFT calculation for Cs and Sr ion respectively. **c**. Plot of calculated binding energy (BE) versus ring size of substituted crown ether at same level of theory as in Fig. 6a in metal ion- crown ether complexes. Filled black square and circle represent the results obtained from the present DFT calculation for Cs and Sr ion respectively

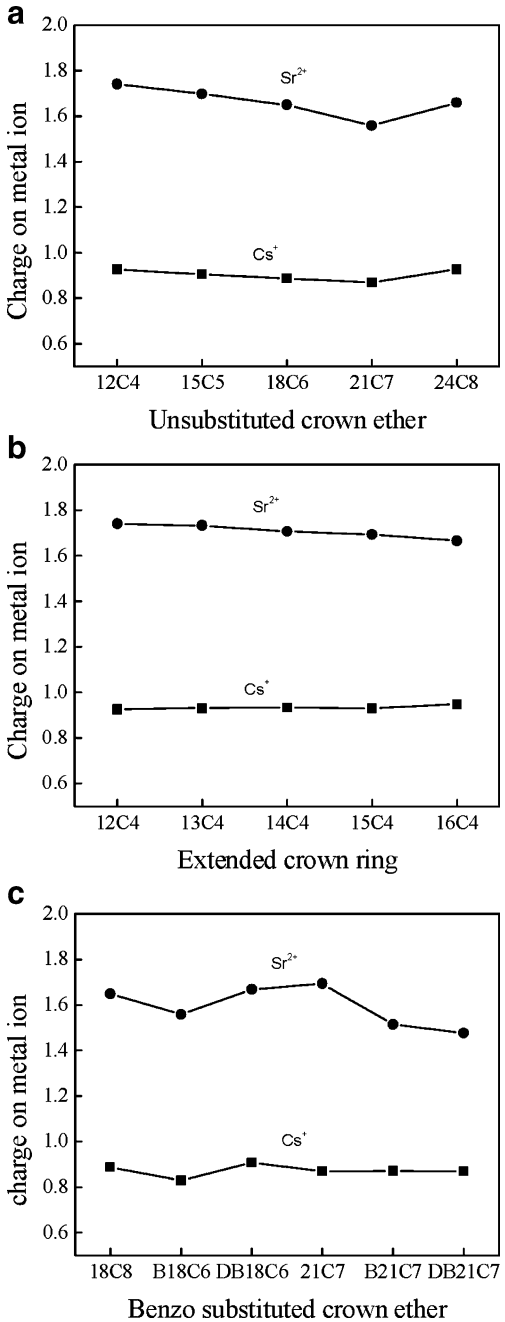

Fig. 7 **a**. Plot of calculated charge on metal ion versus ring size of unsubstituted crown ether at same level of theory as in Fig. 6a. Filled black square and circle represent the results obtained from the present DFT calculation for Cs and Sr ion respectively. **b**. Plot of calculated charge on metal ion versus ring size of extended crown ether at same level of theory as in Fig. 6a. Filled black square and circle represent the results obtained from the present DFT calculation for Cs and Sr ion respectively. **c**. Plot of calculated charge on metal ion versus ring size of substituted crown ether at same level of theory as in Fig. 6a. Filled black square and circle represent the results obtained from the present DFT calculation for Cs and Sr ion respectively

from Fig. 7c. The interaction energy of strontium ion with crown ethers is always higher than cesium ion due to higher charge than cesium ion. The interaction energy is decreased by 8% for Cs^+ ion and 2.58% for Sr^{2+} in going from 18C6 to B18C6. Addition of two phenyl ring in 18C6 reduces the interaction energy by 8.48% for Cs^+ ion and 5.09% for Sr^{2+}. The interaction energy is increased by 2.72% for Cs^+ ion and 4.45% for Sr^{2+} in going from 21C7 to B21C7. The interaction energy is decreased by 8% after addition of two phenyl rings in 21C7 for Cs metal ion but remains almost unchanged for Sr^{2+} metal ions.

The effect of micro-solvation on the binding ability of metal ions with crown ethers (DB18C6 and DB21C7) also has been studied. The binding interaction of metal ions with crown ethers decreases due to the presence of water molecules in the complexes as revealed from values of binding energy given in Table 3. These findings are correlated with the charge on the metal ion from Mulliken population analysis given in Table 3. The transfer of charge from the metal ion to the ligating species is highest for metal ion–ligand complex and is lowest for metal ion-water complex. The charge transfer from the metal ions in micro-solvated metal ion-ligand complexes is higher than that of metal ion-water clusters but lower than that of gas phase metal ion-crown ether complexes.

Quantum chemical descriptors for crown ethers

DFT has an extra-ordinary potential for calculating global and local indices that describe the inherent reactivity of chemical species quantitatively and is thus very useful to describe the host (crown ether) guest (metal ion) type interaction. Chemical systems are generally characterized by their electronic chemical potential, μ and absolute hardness, η and are defined as: [92]

$$-\mu = (\mathrm{I}+\mathrm{A})/2 = \chi \quad \eta = (\mathrm{I}-\mathrm{A})/2 \tag{7}$$

where I is the ionization potential and A is the electron affinity. Here, χ is called the absolute electronegativity. According to Koopmans' theorem [75], I and A can be obtained as:

$$\mathrm{I} = -\mathrm{E_{HOMO}} \quad \mathrm{A} = -\mathrm{E_{LUMO}}\,. \tag{8}$$

If donor acceptor system is brought together, electrons will flow from that of lower χ to that of higher χ, until the chemical potentials become equal. The amount of charge transfer, ΔN can be calculated by applying the following formula: [93]

$$\Delta\mathrm{N} = (\chi_\mathrm{M} - \chi_\mathrm{L})/\{2(\eta_\mathrm{M} + \eta_\mathrm{L})\}. \tag{9}$$

Here, M stands for metal ion, which acts as Lewis acid, i.e., acceptor and L stands for crown ether, which acts as Lewis base, i.e., donor.

A higher value of E_{HOMO} indicates a tendency of the molecule to donate electrons to appropriate acceptor molecule of low empty molecular orbital energy. On the other hand, the energy of the lowest unoccupied molecular orbital indicates the ability of the molecule to accept electrons. Larger values of the energy difference, $\Delta E = E_{LUMO} - E_{HOMO}$, provide low reactivity to a chemical species and lower values of the energy difference indicates higher reactivity.

The calculated values of HOMO and LUMO energies, energy gaps, absolute hardness (η), absolute electro negativity (χ) and charge transfer, ΔN of the optimized crown ligand –metal ion systems are given in Table 6. The HOMO-LUMO energy gaps are decreased gradually from 12C4 to 24C8 except 21C7. The effect of methylene spacers on HOMO and LUMO energies and energy gaps in going from 12C4 to 16C4 is not very pronounced. The HOMO-LUMO energy gaps are decreased gradually from 12C4 to 16C4 except 14C4. As observed earlier, 12C4 has the largest energy gap among the homologues and hence most stable. The introduction of the phenyl rings to 18C6 and 21C7 is quite substantial and increased the energy of HOMO, decreased the energy of LUMO and energy gaps, which indicates the higher reactivity of the molecule. In order to calculate the fractions of electron transferred from the donor crown ether to the metal ion, theoretical values for absolute electronegativity and absolute hardness for Cs and Sr metal ions were calculated. The theoretical values of absolute electronegativity of Cs and Sr metal ions are 12.28ev and 25.29ev and absolute hardness are 7.38ev and 12.54ev respectively. This indicates that Cs metal ion is soft acid and Sr metal ion is hard acid.

According to Pearson's HSAB principle, hard acids prefer to bind to hard bases and soft acids prefer to bind to soft bases. Crown ether ligand with oxygen as donor atom acts as a hard base as evident from high energy HOMO and high values of hardness (η) and electro negativity (χ). Hence in accordance with the HSAB principle crown ether prefers Sr metal ion over Cs metal ion during complexation.

A large value of ΔN is favorable for a donor-acceptor reaction. The value of ΔN is higher for Sr^{2+}-crown ether system than Cs^+-crown ether system, which indicates that the complexation with Sr metal ion is more favorable than Cs metal ion. The fraction of electron transferred is largest for B18C6 followed by DB18C6, DB21C7 and B21C7 for both Cs and Sr metal ions. The lowest electron transfer is observed in case of complexation with 24C8. From Mulliken population analysis it was found that the charge transfer was highest for 21C7 followed by DB217 and then B21C7 for Cs metal ion, whereas the charge transfer was highest for DB21C7 followed by B21C7 and then 21C7 for Sr metal ion. As stated earlier the binding energy can be correlated

Table 6 Energies of HOMO, LUMO, HOMO-LUMO gap and quantum chemical descriptors for different ligand systems at B3LYP level of theory using cc-PVDZ basis function for H and O atom, cc-PVTZ basis function for C atom

System	E_{HOMO} (ev)	E_{LUMO} (ev)	ΔE (ev)	η	χ	ΔN (w.r.t. Cs^+)	ΔN (w.r.t. Sr^{2+})
Unsubstituted crown ether							
12C4	-6.585	1.785	8.370	4.185	2.40	0.4274	0.6845
15C5	-6.653	1.327	7.980	3.990	2.663	0.4232	0.6847
18C6	-6.609	0.889	7.498	3.749	2.859	0.4227	0.6882
21C7	-6.549	1.344	7.893	3.946	2.602	0.4275	0.6883
24C8	-7.012	0.400	7.412	3.706	3.306	0.4050	0.6768
Extended crown ether							
13C4	-6.484	1.597	8.081	4.040	2.443	0.4309	0.6892
14C4	-6.615	1.526	8.141	4.070	2.544	0.4254	0.6849
15C4	-6.585	1.414	7.999	3.999	2.585	0.4262	0.6866
16C4	-6.729	1.091	7.820	3.910	2.819	0.4192	0.6832
Benzo substituted crown ether							
B18C6	-5.401	0.231	5.632	2.816	2.585	0.4757	0.7395
B21C7	-6.100	-1.080	5.020	2.510	3.590	0.4396	0.7212
DB18C6	-5.450	0.214	5.664	2.832	2.618	0.4733	0.7377
DB21C7	-5.899	-1.074	4.825	2.412	3.486	0.4493	0.7294

with Mulliken charge transfer but no such correlation is obtained with the fraction of electron transfer, ΔN.

Thermodynamic parameters

The binding enthalpy (ΔH) and binding free energy (ΔG) for the metal ion-crown ether complexation reaction in Eq. 1 are calculated using the following standard thermodynamic relation:

$$\Delta H = \Delta U + \Delta nRT. \quad (10)$$

$$\Delta G = \Delta H - T\Delta S. \quad (11)$$

Calculated values of thermodynamic parameters, such as binding enthalpy, free energy of complexation and entropy of complexation (ΔS) are listed in Table 7. These thermodynamic values provide information about the relative stability of crown ether complexes. Formation of metal ion complexes is exothermic as revealed from values of ΔH given in Table 7. The binding enthalpy is increased with increase in the cavity size, i.e., with increase in number of O atoms. The zero point energy and thermodynamical corrected binding energy are calculated from the hessian of the optimized geometry. The binding enthalpy for Sr metal ion is much higher than the Cs metal ion for all the crown ethers studied here. The extended ring is not suitable for Cs^+ metal ion as the binding enthalpy deceases for this extended crown system. In the case of Sr, though the binding enthalpy increases the increment is small in comparison to the benzo substituted crown ether. The free energy change for binding the metal ion is highest for B21C7 with both the Cs^+ and Sr^{2+} metal ions. The calculated values of binding enthalpy of Cs metal ion with the crown ethers are in good agreement with the experimental results [94]. The entropy change for the complexation reaction is slightly negative. However, the change in the enthalpy was large and negative enough to overcome the negative entropy change. From the free energy of complexation it is found that the metal ion-crown ether

Table 7 Calculated thermodynamics parameters and free energy for ion exchange reaction in gas phase and solvent phase at B3LYP level of theory using cc-PVDZ basis function for H and O atom, cc-PVTZ basis function for C atom and 3-21G basis function for Cs and Sr atom. The temperature taken is 298.15 K

System	Cs^+		Sr^{2+}		ΔG_r	logK
	U(a.u)	S ($cal.mol^{-1}K^{-1}$)	U(a.u)	S ($cal.mol^{-1}K^{-1}$)		
M^{n+}-$(H_2O)_6$	-7991.08435	125.55				
M^{n+}- $(H_2O)_8$			-3729.26969	139.41		
M^{n+}-DB18C6	-8759.60998	176.36	-4345.05667	167.73	-127.41	93.73
M^{n+}-DB21C7	-8915.47077	190.60	-4500.96159	175.00	-153.02	112.57
M^{n+}-DB18C6-$(H_2O)_2$			-4497.82560	194.62	-20.31	14.94
M^{n+}-DB21C7-$(H_2O)_2$			-4653.70853	208.49	-34.09	25.08

complexes are readily formed and stable. The binding enthalpy for the metal ions in micro-solvated metal ion-crown complexes is higher than that of hydrated metal ion clusters but smaller than that of metal ion-crown ether complexes in gas phase as clear from the listed values in Table 7.

Selectivity

Gas phase

The metal ion exchange reaction with crown ethers in gas phase can be described as:

$$Cs^{+} - L + Sr^{2+} = Sr^{2+} - L + Cs^{+} \quad (12)$$

In the above exchange reaction the free energy change for the forward reaction is always negative which means the selectivity of Sr^{2+} ion over Cs^{+} ion is always greater in gas phase. The calculated values of exchange free energy and logK for DB18C6 and DB21C7 are given in Table 7.

Micro-solvated metal ion

To study the selectivity of metal ion in the presence of solvent water molecules, we have considered the same exchange reaction but in presence of micro-solvated metal ions by the following exchange reaction:

$$Cs^{+} - L + Sr^{2+}(H_2O)_8 = Sr^{2+} - L - (H_2O)_2 + Cs^{+} - (H_2O)_6. \quad (13)$$

The change in free energy and also the equilibrium constant for the above exchange reaction for DB18C6 and DB21C7 are reported in Table 7. Only DB18C6 and DB21C7 were considered for study due to its higher partition coefficients than 18C6, 21C7, B18C6 and B21C7 [95]. The calculated value of exchange free energy for DB18C6 and DB21C7 favors the selection of Sr^{2+} ion over Cs^{+} ion in presence of solvent water as revealed from the high logK value. The present study demonstrates that the binding and the preferential selectivity of the metal ion are basically decided by the number of electron donor sites within the ring, donor atom basicity, size of the crown ether cavity and metal ion, charge on the guest metal ion, presence of solvent, donor-cation distance and orientation of the donor dipoles. Micro-solvation of the metal ions and metal ion-crown ether complexes also changes the binding interaction of metal ions with crown ethers. The free energy change for the ion exchange reaction in the gas phase is altered due to micro-solvation of the metal ions.

IR frequency of hydrated metal ion-crown ether complexes

To demonstrate the presence of hydrated metal ion during transfer of metal ions from an aqueous to crown ether containing organic phase it is of great importance to study the O-H stretching frequency of H_2O in the IR spectra of hydrated metal ion-crown ether complexes. DB18C6 and DB21C7 crown ethers were taken for this study. The IR spectra for hydrated metal ion-crown ether complexes are calculated at B3LYP level of theory using Lorentzian line shape with peak half-width of 20 cm^{-1} and values are given in Table 8. The reported experimental vibrational frequencies of H_2O molecule are 1595, 3657 and 3756 cm^{-1} [96]. Based on this reported value on stretching frequency of H_2O and the present calculated values ν_{sym} =3737 cm^{-1}, ν_{asym} =3821 cm^{-1} at B3LYP level, the scaling factor is taken as 0.98 to take care of anharmonicity of stretching vibrations. The scaled IR intensity for hydrated strontium metal ion and hydrated strontium metal ion-crown complexes is plotted against wave number and is displayed in Fig. 8. IR spectra of di-hydrated crown ether complexes of strontium metal ion are distinctly different than the corresponding hydrated metal ion without crown ether. The anti symmetric stretching frequency in di-hydrated strontium metal ion-DB18C6 crown complex is the same as in the di-hydrated strontium metal ion-DB21C7 crown complex but there is a blue shift in symmetric stretching frequency as one goes from di-hydrated strontium metal ion-DB18C6 crown complex to di-hydrated strontium metal ion-

Table 8 Calculated scaled O–H stretching frequency of H_2O in hydrated metal ion-crown ligand complex at B3LYP level of theory using cc-PVDZ basis function for H and O atom, cc-PVTZ basis function for C atom and 3-21G basis function for Sr atom. The anharmonic nature of stretching frequency is taken care of by applying a scaling factor of 0.98. This scaling factor is calculated based on experimental and present calculated values for O-H stretching frequency of water

System	ν_{OH}(symmetric) cm^{-1}	ν_{OH}(anti symmetric) cm^{-1}
H2O	3662(3657*)	3745(3756*)
Sr^{2+}-H_2O	3688	3719
Sr^{2+}-2H_2O	3688, 3699	3772, 3740
DB18C6-Sr^{2+}-2H_2O	3748, 3749	3823, 3831
DB21C7-Sr^{2+}-2H_2O	3724, 3751	3823,3835

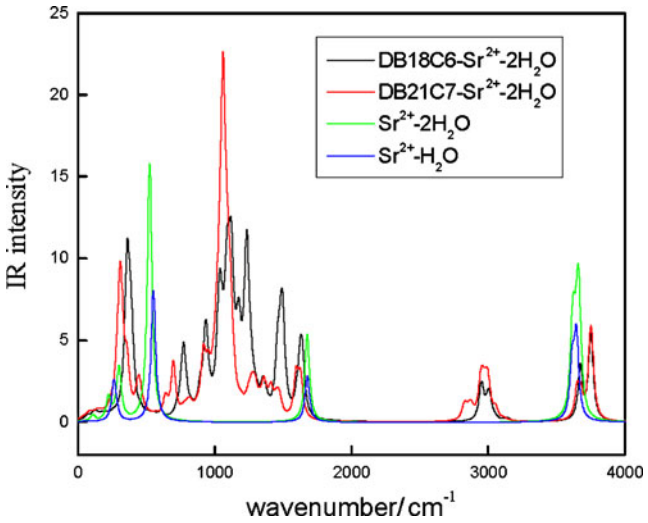

Fig. 8 Calculated scaled IR intensity versus wavenumber of hydrated strontium metal ion and hydrated strontium metal ion crown ether complexes

DB21C7 crown complex. The symmetric and asymmetric stretching bands are shifted to the higher side by 60 and 96 cm^{-1} respectively in hydrated metal ion-DB18C6 crown complex in comparison to the hydrated metal ion, whereas, in hydrated metal ion-DB218C7 crown complex, the shifting in asymmetric stretching band is the same as that of DB18C6-metal ion complex but the symmetric stretching band is reduced by 24 cm^{-1} in comparison to the value of DB18C6-metal ion complex. The calculated IR frequencies will help to determine the presence of micro-solvated metal ion in metal ion-crown ether complexes in extractant phase. We are not aware of any experimentally reported IR results for comparing our calculated results and hence experimental work is invited to test the predicted results.

It is to be noted that experimental works for the estimation of IR spectra of hydrated alkali metal ion-crown complex has been recently reported using IPRD technique [97].

Conclusions

The cavity size was predicted from the optimized geometries of various crown ethers based on B3LYP calculations within the framework of DFT. The cavity size is increased from 12C4 to 21C7 and 12C4 to 16C4 but is decreased from 18C6 to 21C7 when it is substituted by phenyl rings. The calculated values of binding energy is enhanced from 12C4 to 21C7 and then reduced in 24C8 crown for both Cs^+ and Sr^{2+} metal cations. The predicted values of binding energy are decreased from 12C4 to 16C4 with Cs^+ metal ion whereas increased with Sr^{2+} metal ion. The calculated values of binding energy is decreased from 18C6 < B18C6 < DB18C6 for both Cs and Sr metal ions. In going from 21C7 to DB21C7, the binding energy is decreased due to the electron withdrawing and resonance effect of the phenyl ring. The introduction of the phenyl rings to 18C6 and 21C7 is quite substantial and increased the energy of HOMO, decreased the energy of LUMO and energy gaps, which indicates the higher reactivity of the donor crown molecule. Suitable ligand architecture is predicted for Cs^+ and Sr^{2+} ion using the optimized structures of various free macrocyclic crown ethers and its complexes with Cs^+ and Sr^{2+} metal ions. The selectivity of Cs^+ and Sr^{2+} for a particular size of crown ether is explained based on the fitting of the guest metal ion within the narrow cavity of the host crown ether, binding enthalpy and molecular descriptors. The replacement of $–CH_2-CH_2-$ linkage in ring with phenyl leads to the reduction of the crown cavity volume and hence imparts rigidity to the ligand and thus causing the reduction in the cavity size, whereas $-CH_2-CH_2-CH_2-$ unit inside the ring expands the cavity size of the basic crown ether. Though, it is established that Cs^+ ion nicely fits in the cavity of Di-Benzo-21-Crown-7 and Sr^{2+} ion in the cavity of Di-Benzo-18-Crown-6, both crown ethers pick up Sr^{2+} ion from a mixture of Cs^+ and Sr^{2+} metal ions based on the values of free energy of ion exchange reaction. In C4 homologues series, 15C4 shows the maximum binding energy for both the Cs^+ and Sr^{2+} metal ions. The extended ring is not suitable for Cs^+ metal ion as the binding energy is decreased for this extended crown system. The free energy change for binding the metal ion is highest for B21C7 with both the Cs^+ and Sr^{2+} metal ions. The calculated values of binding enthalpy of Cs metal ion with the crown ethers are in good agreement with the experimental results. In the case of Sr, though the binding energy is increased, the increment is low in comparison to benzo substituted crown ether. Thus, quantum chemistry based molecular modeling approach can be used to design a ligand molecule for a specific metal ion of interest. The calculated IR spectra can be compared with an experimental spectrum to determine the presence of micro-solvated metal ion–crown ether complexes in extractant phase. It will be of great importance to study the effect of conformation, DFT functional and basis function on the properties reported here.

Acknowledgments Computer division, Bhbha Atomic Research Centre is greatly acknowledged for providing the parallel computation facility.

References

1. Pederson CJ (1967) J Am Chem Soc 89:7017-7036; (1998) J Angew Chem Int Ed Engl 27:1021-1027
2. Badis M, Tomaszkiewicz I, Joly JP, Rogalska E (2004) Langmuir 20:6259–6267

3. Corvis Y, Korchowiec B, Korchowiec J, Badis M, Mironiuk-Puchalska E, Fokt I, Priebe W, Rogalska E (2008) J Phys Chem B 112:10953–10963
4. Izatt RM, Bradshaw JS, Nielsen SA, Lamb JD, Christensen JJ, Sen D (1985) Chem Rev 85:271–339
5. Izatt RM, Pawlak K, Bradshaw JS, Bruening RL (1991) Chem Rev 91:1721–2085
6. Gokel GW (1991) Crown ethers and cryptands. The Royal Society of Chemistry, London
7. Sannicolo F, Brenna E, Benincori T, Zotti G, Zecchin S, Schiavon G, Pilati T (1998) Chem Mater 10:2167–2176
8. Tokunaga Y, Nakamura T, Yoshioka M, Shimomura Y (2006) Tetrahedron Lett 47:5901–5904
9. Mathias LJ (1981) J Macromol Sci Chem A15:853
10. Tran CD, Zhang W (1990) Anal Chem 62:830–834
11. Kuwahara Y, Nagata H, Nishi H, Tanaka Y, Kakehi K (2005) Chromatographia 62:505–510
12. Chen S, Yuan H, Grinberg N, Dovletoglou A, Bicker G (2003) J Liq Chromatogr Relat Technol 26:425–442
13. Munoz S, Mallen J, Nakano A, Chen Z, Gay I, Echegoyen L, Gokel GW (1993) J Am Chem Soc 115:1705–1711
14. Mazik M, Kuschel M, Sicking W (2006) Org Lett 8:855–858
15. Cazacu A, Tong C, Van der Lee A, Fyles TM, Barboiu MJ (2006) J Am Chem Soc 128:9541–9548
16. Puchta R, van Eldik R (2007) Eur J Inorg Chem 10:1120–1127
17. Puchta R, van Eldik R (2008) J Incl Phenom Macrocycl Chem 60:383–392
18. Hancock RD (1993) J Incl Phenom Macrocycl Chem 17:63–80
19. Pearson RG (1963) J Am Chem Soc 85:3533–3539
20. Pearson RG (1966) Science 151:1721–1727
21. Schulz WW, Bray LA (1987) Sep Sci Technol 22:191–214
22. Kinard WK, McDowell WJ, Shoun RR (1980) Sep Sci Technol 15:1013–1024
23. Kinard WK, McDowell WJ (1981) J Inorg Nucl Chem 43:2947–2953
24. McDowell WJ, Moyer BA, Case GN, Case FI (1986) Solvent Extr Ion Exch 4:217–236
25. Blasius E, Nilles KH (1984) Radiochim Acta 35:173–182
26. Shuler RG, Bowers CB Jr, Smith JE, Van Brunt V, Davis MW Jr (1985) Solvent Extr Ion Exch 3:567–604
27. McDowell WJ (1988) Sep Sci Technol 23:1251–1268
28. McDowell WJ, Case GN, McDonough JA, Bartsh R (1992) Anal Chem 64:3013–3017
29. Strzelbickl J, Bartsch RA (1984) Anal Chem 53:1894–1899
30. Brown PR, Bartsch RA (1991) Ion extraction and transport by proton-ionizable crown ethers. In: Osa T, Atwood JL (eds) Inclusion aspects of membrane chemistry. Kluwer, Boston, pp 1–57
31. McDowell WJ, Case GN, Aldrup W (1983) Sep Sci Technol 18:1483–1507
32. Gerow IH, Smith JE Jr, Davis MW Jr (1981) Sep Sci Technol 16:519–548
33. Horwitz EP, Dietz ML, Fisher DE (1990) Solvent Extr Ion Exch 8:199–208
34. Dietz ML, Horwitz E, Rhoads S, Bartsch R, Krzykawski J (1996) Solvent Extr Ion Exch 14:1–12
35. Horwitz EP, Dietz ML, Fisher DE (1990) Solvent Extr Ion Exch 8:557–572
36. Hay BP, Firman TK (2002) Inorg Chem 41:5502–5512
37. Lumetta GJ, Rapko BM, Garza PA, Hay BP (2002) J Am Chem Soc 124:5644–5645
38. Chakraborty A (2001) Advances in chemical engineering, molecular modelling and theory in chemical engineering, vol 28. Academic, New York
39. Cramer CJ (2004) Essentials of computational chemistry, theories and models, 2nd edn. Wiley, New York
40. Liou CC, Brodbelt JS (1992) J Am Chem Soc 114:6761–6764
41. Wu HF, Brodbelt JS (1994) J Am Chem Soc 116:6418–6426
42. Alvarez EJ, Wu HF, Liou CC, Brodbelt JS (1996) J Am Chem Soc 118:9131–9138
43. More MB, Ray D, Armentrout PB (1997) J Phys Chem A 101:831–839
44. Wipff G, Weiner P, Kollman P (1984) J Am Chem Soc 104:3249–3258
45. Hancock RD (1990) Acc Chem Res 23:253–257
46. Howard AE, Singh UC, Billeter M, Kollman PA (1988) J Am Chem Soc 110:6984–6991
47. van Eerden J, Harkema S, Fed D (1988) J Phys Chem 92:5076–5079
48. Straatsma TP, McCammon JA (1989) J Chem Phys 91:3631–3637
49. Dang LX, Kollman P (1990) J Am Chem Soc 112:5716–5720
50. Sun Y, Kollman PA (1992) J Chem Phys 97:5108–5112
51. Leuwerink FTH, Harkema S, Briels WJ, Feil DJ (1993) Comput Chem 14:899–906
52. Ha YL, Chakra Borty AK (1991) J Phys Chem 95:10781–10787
53. Ha YL, Chakraborty AK (1993) J Phys Chem 97:11291–11299
54. Hay BP, Rustad JR (1994) J Am Chem Soc 116:6316–6326
55. Ranghino G, Romano S, Lehn JM, Wipff G (1985) J Am Chem Soc 107:7873–7877
56. Jagannadh B, Jagarlapudi A, Sarma RP (1999) J Phys Chem A 103:10993–10997
57. El-Azhary AA, Al-Kahtani AA (2004) J Phys Chem A 108:9601–9607
58. Seidl ED, Schafer HF III (1991) J Phys Chem 95:3589–3590
59. Wasada H, Tsutsui Y, Yamane S (1996) J Phys Chem 100:7367–7371
60. Hill SE, Feller D, Glendenning ED (1998) J Phys Chem 102:3813–3819
61. Yamabe T, Hori K, Akagi K, Fukui K (1979) Tetrahedron 35:1065–1072
62. Hori K, Yamada H, Yamabe T (1983) Tetrahedron 39:67–73
63. Ha YL, Chakraborty AK (1992) J Phys Chem 96:6410–6417
64. Glendening ED, Feller D, Thompson MA (1994) J Am Chem Soc 116:10657–10669
65. Glendening ED, Feller D (1996) J Am Chem Soc 118:6052–6059
66. Feller D (1997) J Phys Chem A 101:2723–2731
67. Feller D, Apra E, Nichols JA, Bernholdt DE (1996) J Chem Phys 105:1940–1950
68. Feller D, Thompson MA, Kendall RA (1997) J Phys Chem A 101:7292–7298
69. Cui C, Cho SJ, Kim KS (1998) J Phys Chem A 102:1119–1123
70. Tossel JA (2001) J Phys Chem B 105:11060–11066
71. De S, Ali SM, Shenoi MRK, Ghosh SK, Maity DK (2009) Desalin Water Treat 12:93–99
72. Hill SE, Feller D (2000) Int J Mass Spectrom 201:41–58
73. Nicholas JB, Hay BP (1999) J Phys Chem A 103:9815–9820
74. Dearden DV, Paulsen ES, Anderson JD (2003) Int J Mass Spectrom 227:63–67
75. Parr RG, Yang W (1989) Density functional theory of atom and molecules. Oxford University Press, New York
76. Becke AD (1993) J Chem Phys 98:5648–5652
77. Olletta AC, Lee HM, Kim KS (2006) J Chem Phys 124:0243211–0243213
78. Ali M, Maity DK, Das D, Mukherjee T (2006) J Chem Phys 124:0243251–0243257
79. Ali SM, Maity DK, De S, Shenoi MRK (2008) Desalination 232:181–190
80. Ali SM, De S, Maity DK (2007) J Chem Phys 127:044303–044311
81. Schmidt MW, Baldridge KK, Boatz JA (1993) J Comput Chem 14:1347–1363
82. Schaftenaar G, Noordik JH (2000) J Comput-Aided Mol Des 14:123–134

83. Boys SF, Bernardi F (1970) Mol Phys 19:553–566
84. Scotto MA, Mallet G, Vasilescu D (2005) J Mol Struct THEOCHEM 728:231–242
85. De S, Ali SM, Ali A, Gaikar VG (2009) Phys Chem Chem Phys 11:8285–8294
86. De S, Boda A, Ali SM (2010) J Mol Struct THEOCHEM 941:90–101
87. Hou H, Zeng X, Liu X (2009) J Mol Model 15:105–111
88. Jensen MP, Dzielawa JA, Rickert P, Dietz ML (2002) J Am Chem Soc 124:10664–10665
89. Anil Kumar AV, Bhatia SK (January, 2007) Australian patent WO 2007/000027 A1, 4
90. Steed JW (2001) Coord Chem Rev 215:171–221
91. Maheswari S, Patel N, Satyamurty N, Kulkarni AD, Gadre SR (2001) J Phys Chem A 105:10525–10537
92. Pearson RG (1988) Inorg Chem 27:734–740
93. Parr RG, Pearson RG (1983) J Am Chem Soc 105:7512–7516
94. Joseph DA, Eric SP, David VD (2003) Int J Mass Spectrom 227:63
95. Boda A, Ali SM, Shenoi MRK (2010) Fluid Phase Equilib 288:111–120
96. Hoy AR, Mills IM, Strey G (1972) Mol Phys 24:1265–1290
97. Rodriguez JD, Vaden TD, Lisy JM (2009) J Am Chem Soc 131:17277–17288
98. Malgorzata U, Walkowiak W, Bartsch RA (2006) Sep Purif Technol 48:264–269